

The Mott metal-insulator transition in half-filled two-dimensional Hubbard models

Peyman Sahebsara

Département de Physique and Regroupement Québécois sur les Matériaux de Pointe,
 Université de Sherbrooke, Sherbrooke, Québec, Canada, J1K 2R1

(Received 22 January 2008 ; in final form 19 April 2008)

Abstract

We study the Mott transition in the two dimensional Hubbard model by using the variational cluster approximation. The transition potential obtained is roughly $U_c \approx 2$ and 6 for square and triangular lattices, respectively. A comparison between results of this approximation and other quantum cluster methods is presented. Our zero-temperature calculation at strong coupling show that the transition on the triangular and square lattices occur at lower values of U compared with other numerical techniques such as DMFT, CDMFT, and DCA. We also study the thermodynamic limit by an extrapolation to infinite size.

Keywords: Hubbard model, Mott transition, VCA, spectral function, density of states, quantum cluster methods

1. Introduction

The Mott metal-insulator transition is one of the most fascinating subjects in condensed matter physics. The independent electron approach explains the metallic and insulating phases just by looking at the filling of the electronic bands. Taking electron-electron interactions into account in a perturbative way just leads to a renormalization of energy bands, and cannot by itself induce a transition between a metal and an insulator. However, many transition-metal compounds are insulators, whereas they are predicted to be metallic by the band approach. The insulating behavior in strongly correlated materials was explained by Mott in his pioneering paper [1], as the result of the competition between two opposite tendencies: (i) the localization of electrons on the lattice due to their Coulombic repulsion and (ii) their hopping between neighboring sites. Accordingly, these systems are called “Mott insulators”. For further background on the Mott transition, readers are referred to the review paper by Imada [2].

The physics of the Mott transition in two-dimensional systems has been studied theoretically mainly on simple Hubbard models defined on the square and triangular lattices. In such systems, the Mott phase is in competition with magnetically ordered phases, that are also insulating, although because of a seemingly different mechanism, related to the presence of a magnetic unit cell and of the associated band gap. Since

the Mott gap is smaller than the AF gap and the U_c of the Mott insulating phase is smaller than the critical U of the AF insulating phase, the Mott gap is often masked by this ordering gap. However, understanding the nature of the Mott gap is important since it usually accompanies other critical phases such as superconducting and spin liquid states. Moreover, the value of the critical interaction strength U_c at zero temperature is an important characteristic of the transition.

Examples of quasi-two-dimensional systems that are studied using the Hubbard model are high temperature cuprate superconductors and layered organic superconductors, which all have rich ground state phase diagrams. In cuprates, a transition from a Néel antiferromagnetic insulator to a superconducting phase is induced upon doping [3]. A very similar phase diagram has been obtained by applying pressure to organic compounds at half-filling, such as κ -(BEDT-TTF)₂Cu₂(CN)₈ and EtMe₃Sb[Pd(dmit)₂]₂ [4, 5, 6, 7, 8].

The Mott transition on the 2D Hubbard model has been studied using several analytical and numerical methods: a dynamical Mean field theory (DMFT) [9, 10], a dynamical cluster approximation (DCA) [11], a variational cluster approximation (VCA) [12, 13], and a cellular dynamical mean field theory (CDMFT) [15, 28]. This paper is organized as follows. In the next section a short introduction to the 2D Hubbard model will be given, followed by a brief discussion about the

variational cluster approximation, the method used in this paper. We then review cluster extensions of dynamical mean field theory. The next section describes our numerical results, which are compared with those of other methods.

2. Model and formalism

We consider the single-band Hubbard model, with nearest neighbor hopping t , as the minimum model required to study the Mott-Hubbard transition:

$$H = - \sum_{i,j,\sigma} t_{ij} c_{i\sigma}^\dagger c_{j\sigma} + U \sum_i n_{i\uparrow} n_{i\downarrow}, \quad (1)$$

where $c_{i\sigma}^\dagger$ is the creation operator for electrons of spin σ , $n_{i\sigma} = c_{i\sigma}^\dagger c_{i\sigma}$ is the density of electrons, t_{ij} is the hopping amplitude between sites i and j , and U is the on-site Coulomb repulsion. The Mott transition is driven by the competition between the hopping amplitudes and U . The kinetic part of the model, based on electrons hopping on a lattice within a tight-binding scheme, tends to delocalize the electrons, which favors a metallic state. On the other hand, the potential part based on the on-site Coulomb repulsive term tends to localize the electrons in order to avoid double occupancies, and so favors an insulating state at half filling.

Despite its simplicity, the two-dimensional Hubbard model contains the most relevant terms to understand the role of electron correlations and is extremely difficult to investigate. Except for the one-dimensional case with nearest-neighbor hopping, an exact solution is not available. In recent years a number of numerical methods have been applied to the Mott transition in the Hubbard model. Among those, quantum cluster methods are based on the exact solution of the model on a finite cluster of sites, and use a procedure to take into account the effect, on the cluster, of the infinite lattice. These approaches use numerical methods such as exact diagonalizations (ED) or quantum Monte-Carlo (QMC) to solve the model on the finite cluster (the so-called *impurity model*). Spatial correlations within the cluster are treated accurately, while long range physics is described at the mean field level. In those methods, the irreducible self-energy of the cluster is used as an approximation for the lattice self-energy, from which an approximate lattice Green function is calculated. In this paper we will describe the results obtained from the Variational Cluster Approximation (VCA).

VCA is an extension of Cluster Perturbation Theory (CPT) that allows for broken symmetry states. CPT [16, 17] is a cluster extension of the strong-coupling expansion of the Hubbard model. The first step in the CPT is to divide the original lattice into finite clusters. The cluster Green function is calculated exactly whereas the hopping between adjacent clusters is taken into account perturbatively at the lowest order. An approximate single-electron Green function at arbitrary values of the wave vector in the Brillouin zone can then

be calculated. It becomes exact in the limit of infinite cluster size, or in the strong or weak coupling limit.

VCA allows broken-symmetry phases by adding Weiss field to the cluster Hamiltonian, while at the same time subtracting them at lowest order in strong-coupling perturbation theory. The precise value of the Weiss field is set by minimizing the resulting grand potential [18]. This procedure, apparently heuristic, can be formally justified by Potthoff's self-energy-functional theory (SFT) [19, 20]. For a system with Hamiltonian $H = H_0(t) + H_1(U)$ the grand potential is finally written as function of physical parameters:

$$\Omega(t') = \Omega' + \text{Tr} \ln(G_0^{-1} - \Sigma)^{-1} - \text{Tr} \ln(G'), \quad (2)$$

where $G_0 = (\omega + \mu - t)^{-1}$ is the free Green function of the original model in the thermodynamic limit at frequency ω . Ω' , Σ , and G' are the grand potential, the self-energy, and the Green function of the cluster reference system which depend on the one-particle parameters t' (including Weiss fields) [20]. The stationary points of the function (2) - obtained by numerically solving $\partial\Omega/\partial t' = 0$ - provides a good approximation to the exact solution for the system. In practice, only the Weiss field parameters and the cluster chemical potential are used as variational parameters within the set t' .

VCA was used successfully to study ordered phase in 2D systems. For instance it has recently been used to investigate the competition between Néel antiferromagnetism (AF) and d -wave superconductivity (d -SC) in cuprates [21, 22] and in layered organic compounds [23, 24]. It was also used to study the range of magnetic spiral ordering (MSO) in the triangular-lattice Hubbard model [12].

Other quantum cluster methods (DCA and CDMFT) are extensions of Dynamical Mean Field Theory (DMFT). DMFT provides a description of the Mott transition in the Hubbard model that is exact in infinite dimension [25]. It maps the lattice problem to a single correlated site (the so-called *impurity*) embedded in a surrounding host whose parameters must be determined self-consistently. Thus DMFT neglects spatial correlations. To describe non-local order parameters, it is crucial to add lattice effects to DMFT. In DCA, the DMFT single site is replaced by a finite cluster treated in momentum space: The first Brillouin zone is decomposed into N_c equal cells. In two dimensions, this is equivalent to tiling the original N -site lattice by N/N_c clusters of size $N_c = L \times L$ embedded in a self-consistent effective medium. This approximation assumes that the lattice self-energy is weakly momentum dependent, and becomes exact for an infinite cluster size. The cluster problem in DCA is usually solved by quantum Monte-Carlo (QMC) simulations.

Like DCA, CDMFT maps a lattice problem onto a finite size cluster, this time with open boundary conditions. However, CDMFT can be described in the

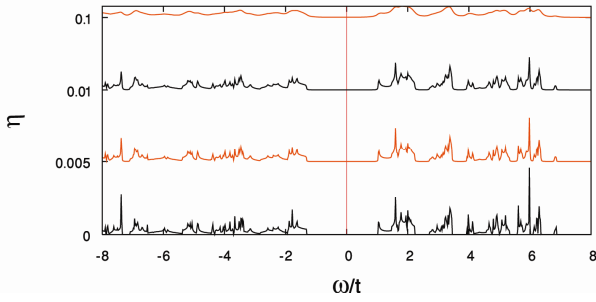


Figure 1. (color online) The density of states, calculated for 3 finite values of η (the imaginary part of the frequency), on a 6-site isotropic triangular cluster at $U=8$. A pointwise extrapolation of these curves is used to obtain the curve at $\eta=0$.

framework of Potthoff's self-energy functional approximation (SFA), like VCA. The solution to the cluster problem are customarily obtained by QMC (at finite temperature) or exact diagonalization (at zero temperature). In the zero-temperature case, the "host" is represented by a bath of non correlated sites that exchanges electrons with the cluster. The bath parameters (site energies and hybridization to the cluster) are determined self-consistently.

3. Numerical results

The Mott transition can be studied by looking at the density of states (DOS), which is the momentum-integrated spectral function:

$$\begin{aligned} \rho(\omega) &= \sum_{\mathbf{k}} A(\mathbf{k}, \omega) \\ &= -\frac{1}{\pi} \lim_{\eta \rightarrow 0^+} \sum_{\mathbf{k}} \Im G(\mathbf{k}, \omega + i\eta), \end{aligned} \quad (3)$$

where \mathbf{k} is the wave vector, ω frequency, and $A(\mathbf{k}, \omega)$ is the single-particle spectral function (imaginary part of the single particle Green function). Close to the transition, the DOS shows the Mott gap more clearly than the spectral function, although the latter is more useful to study the pseudogap phenomenon or gaps caused by broken symmetries[23].

Before presenting our results for density of states, a few points should be mentioned about the numerical technique we use. In our calculations by VCA we adjust the chemical potential to keep the total occupation at half-filling. Note that in calculating the density of states, there is no distinction between VCA and CPT. The calculations are all done at zero temperature. To obtain the DOS using the Green function through Eq. 3 we initially calculate the corresponding densities for a few values of the imaginary part of the frequency (η). Then results are simply extrapolated pointwise to $\eta \rightarrow 0$ (Fig. 1). In this way one avoids the problems associated with the presence of sharp peaks close to $\eta=0$, which make the momentum integrals longer because of adaptive re-meshing. The DOS at $\eta=0$ (shown in the bottom curve of Fig. 1 is obtained by extrapolating from the three values $\eta=0.1$, 0.01, and 0.005. It can be

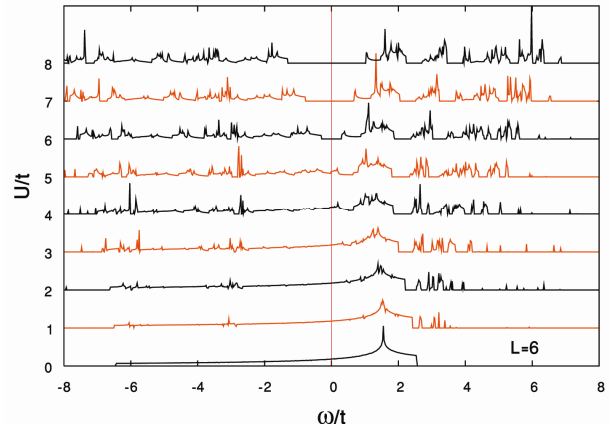


Figure 2. (color online) The evolution of the density of states as a function of interaction U/t , for a 6-site triangular cluster.

seen that the main (overall broad) features can be seen even at large η , however the precise value of the Mott gap can be obtained from this extrapolation.

To find the critical interaction U_c , one can look at the evolution of the DOS as a function of U . Fig. 2 illustrates this evolution for the 6-site cluster. This is one of clusters that have been used to study the magnetic spiral order[12]. Note that in the triangular system, the Van Hove singularity is no longer found at the center of the band, as can be seen on the lowest curve of Fig. 2. From this figure, we see that the Mott gap (for the 6-site cluster) appears between $U=5$ and $U=6$.

The results obtained for clusters of size $L=3$ and $L=15$ - the largest triangular cluster that can be studied with the present computer facilities - show a comparable phase transition[12]. However, the gap corresponding to these finite cluster size can disappear in the thermodynamic limit, due to size effects and boundary conditions. An infinite-size extrapolation of the results can show the existence of the gap. A scaling parameter Q is defined, which is proportional to the number of links in a cluster and has an inverse relation with the total number of links of the original lattice within the unit-cell of the super-lattice of clusters. Q varies from 0 to 1 by increasing the cluster size from single-site to infinite lattice [26]. The evolution of the gap size Δ as a function of cluster size (i.e., of the cluster scaling parameter Q) is shown on the right panel of Fig 3, and indicates that the Mott gap, although decreasing with cluster size, does not vanish in the thermodynamic limit ($Q \rightarrow 1$) for the values of U shown. The left panel of Fig 3 shows the evolution of this gap as a function of U . For all three clusters, the gap vanishes at around $U \approx 6$. This value obtained from VCA is smaller than the results of other methods: the ED on lattice of 12-sites it is $U_c = 12t$ [27], in DMFT+ED $U_c = 15t$ [9], in DMFT+QMC the value is $U_c = 12t$ (finite temperature close to zero) [10]; and CDMFT+ED gives $U_c = 10.5t$ [15].

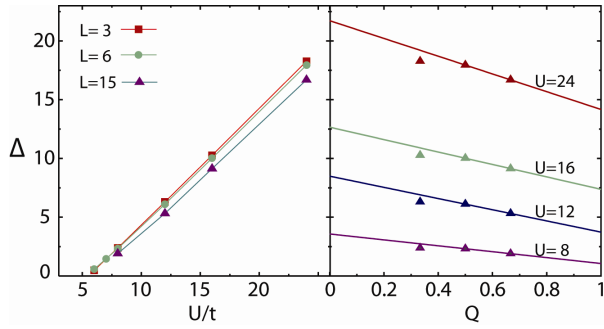


Figure 3. (color online) *Left:* Single particle gap as a function of U for the three clusters used. The metal-insulator transition occurs at $U \approx 6$. *Right:* Single particle gap as a function of cluster scaling parameter Q for several values of U .

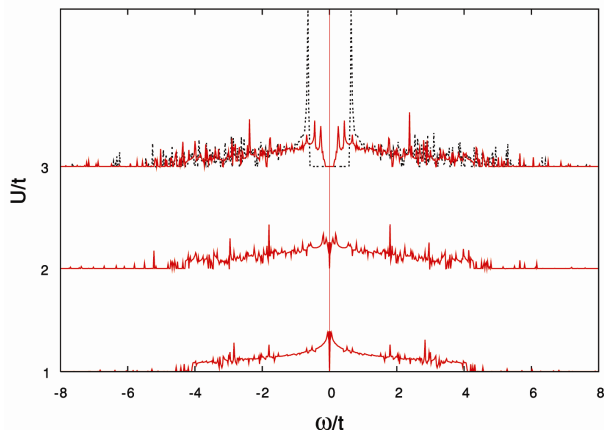


Figure 4. (color online) Density of states calculated from the lattice Green function obtained for a 12-site cluster tiling the square lattice, for 3 values of U/t . Solid curves represent the normal state and dotted line represents the AF ordered system.

Next we obtain the DOS for the square system by the same procedure explained above for the triangular case. Fig. 4 shows the DOS calculated by VCA for three values of U for a 12-sites square cluster. In contrast to the triangular case, the Van Hove peak exists at zero frequency and the distribution is symmetrical about $\omega = 0$. Solid and dotted curves represent the normal and (AF) ordered phase, respectively. One can see that the Mott transition happens around $U/t \approx 2$. Indeed in the same figure we see that the AF gap always masks the Mott gap since it is bigger and consequently the AF transition happens at smaller U/t . Presumably this happens in realistic systems. The Mott transition in the square lattice obtained from VCA has also been discussed in Ref. [13]. In CDMFT the transition happens at $U_c \approx 6t$ [28]. This is a further indication that the Mott transition always happens at a weaker interaction U_c in VCA compared with other methods.

Now we look at the spectral function $A(\mathbf{k}, \omega)$ for the triangular system. Fig. 5 shows the spectral function for a 15-site cluster for two different values of the interaction U/t , above and below the Mott transition.

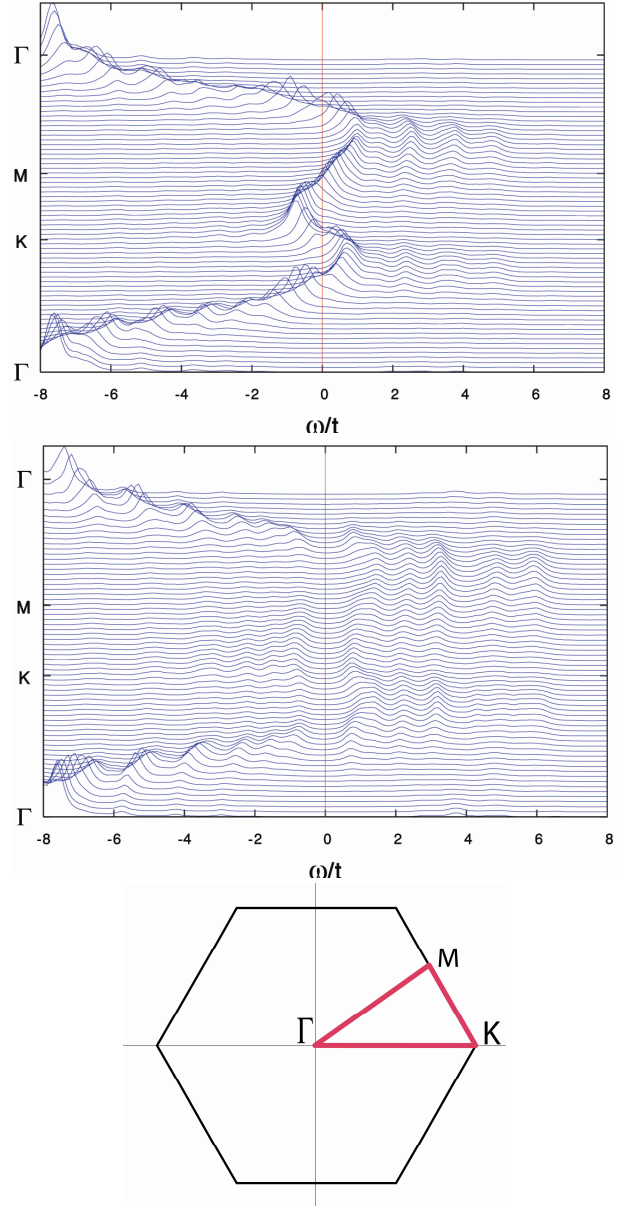


Figure 5. (color online) Single particle spectral weight, as a function of energy ω/t (energy distribution curves) obtained from a 15-site triangular cluster, at $U/t = 5$ (top) and $U/t = 7$ (middle). The vertical line at $\omega = 0$ represents the Fermi level. *bottom:* The first Brillouin zone of the triangular lattice, showing the path used for calculating the spectral function.

On the top panel of the figure $U/t = 5$, and the spectrum looks similar to the non-interacting dispersion. There is no gap and the spectral function represents a metallic phase. At $U/t = 7$ (lower panel) the spectral function loses weight at Fermi level and displays a Mott gap across all wave vectors. This shows that the Mott transition happens between $U/t = 5$ and $U/t = 7$.

4. Conclusion

We have studied the density of states on triangular and square lattices by using the variational cluster approximation on the 2D Hubbard model. The U -

dependence of the extrapolated size of the Mott gap for different clusters was used to obtain the critical value of the interaction at the Mott transition. The VCA estimates the critical interaction for the Mott transition for a triangular lattice roughly to be $U_c \approx 6t$, while in the case of a square lattice this value is around $U_c \approx 2t$. In both cases VCA results are smaller compared with DCA and CDMFT calculations, which shows that VCA relatively tends to exaggerate the transition.

References

1. N F Mott *Proc. Phys. Soc. (London)*, **62** (1949) 416.
2. M Imada, A Fujimori and Y Tokura, *Rev. Mod. Phys.* **70** (1998) 1039.
3. A Damascelli, Z Hussain and Z-X Shen, *Rev. Mod. Phys.* **75** (2003) 473.
4. S Lefebvre, P Wzietek, S Brown, C Bourbonnais, D Jérôme, C Mézière, M Fourmigué and P Batail, *Phys. Rev. Lett.* **85** (2000) 5420.
5. Y Shimizu, K Miyagawa, K Kanoda, M Maesato, and G Saito, *Phys. Rev. Lett.* **91** (2003) 107001.
6. Y Kurosaki, Y Shimizu, K Miyagawa, K Kanoda, and G Saito, *Phys. Rev. Lett.* **95** (2005) 177001.
7. S Ohira, Y Shimizu, K Kanoda, and G Saito, *J. Low. Temp. Phys.* **142** (2006) 153.
8. T Itou, A Oyamada, S Maegawa, M Tamura and R Kato, *J. Phys. Cond. Matt.* **19** (2007) 145247.
9. J Merino, B J Powell and R H McKenzie, *Phys. Rev. B* **73** (2006) 235107.
10. K Aryanpour, W Pickett and T Scalettar, *Phys. Rev. B* **74** (2009) 085117.
11. Y Imai and N Kawakami, *Phys. Rev. B* **65** (2002) 233103.
12. P Sahebsara and D Sénéchal, *Phys. Rev. Lett.* **100** (2008) 136402.
13. A H Nevidomskyy, C Scheiber, D Sénéchal and A.-M S Tremblay, *Phys. Rev. B* **77** (2008) 064427.
14. B Kyung and A-M S Tremblay, *Phys. Rev. Lett.* **97** (2006) 046402.
15. B Kyung, *Phys. Rev. B* **75** (2007) 033102.
16. D Sénéchal, D Perez, M Pioro-Ladriere, *Phys. Rev. Lett.* **84** (2000)522.
17. D Sénéchal, D Perez and D Plouffe, *Phys. Rev. B* **66** (2002) 075129.
18. C Dahnken, M Aichhorn, W Hanke, E Arrigoni and M Potthoff, *Phys. Rev. B* **70** (2004) 245110.
19. M Potthoff, M Aichhorn and C Dahnken, *Phys. Rev. Lett.* **91** (2003) 206402.
20. M Potthoff, *Eur. Phys. J. B* **32** (2003) 429.
21. D Sénéchal, P-L Lavertu, M-A Marois and A-M S Tremblay, *Phys. Rev. Lett.* **94** (2005) 156404.
22. M Aichhorn, E Arrigoni, M Potthoff and W Hanke, *Phys. Rev. B* **74** (2006) 024508.
23. P Sahebsara and D Sénéchal, *Phys. Rev. Lett.* **97** (2006)257004.
24. P Sahebsara and D Sénéchal, *Iranian Journal of Physics Research* **6**, 3 (2006) 179.
25. A Georges, G Kotliar, W Krauth and M J Rozenberg, *Rev. Mod. Phys.* **68** (1996) 13.
26. For more discussions about the validity of Q see Ref. Sahebsara:2007.
27. M Capone, L Capriotti, F Becca and S Caprara, *Phys. Rev. B* **63** (2001) 085104.
28. B Kyung, S S Kancharla, D Sénéchal, A-M S Tremblay, M Civelli and G Kotliar, *Phys. Rev. B* **73** (2006) 165114.

Acknowledgments

We acknowledge valuable discussion with D. Sénéchal, A.-M. Tremblay, S. R. Hassan, and K. Aryanpour, and appreciate D. Sénéchal for the critical reading of the manuscript. This work was supported by NSERC (Canada). Computations were performed on the Dell clusters of the Réseau Québécois de Calcul de haute performance (RQCHP).